PROCEEDINGS OF SCIENCE

The First LHAASO Catalog of Gamma-ray Sources below 25TeV

S.C. Hu,[a,b,c,*] **G.M. Xiang,**[b,d] **M. Zha**[b,c] **and Z.G. Yao**[b,c] **for the LHAASO collaboration**

[a] *Key Laboratory of Particle Astrophyics & Experimental Physics Division & Computing Center, Institute of High Energy Physics, Chinese Academy of Sciences, 100049 Beijing, China*
[b] *University of Chinese Academy of Sciences, 100049 Beijing, China*
[c] *Tianfu Cosmic Ray Research Center, 610000 Chengdu, Sichuan, China*
[d] *Key Laboratory for Research in Galaxies and Cosmology, Shanghai Astronomical Observatory, Chinese Academy of Sciences, 200030 Shanghai, China*
E-mail: hushicong@ihep.ac.cn, gmxiang@ihep.ac.cn, zham@ihep.ac.cn, yaozg@ihep.ac.cn

We report the first catalog of TeV gamma-ray sources realized with the most sensitive wide field-of-view TeV telescope ever built. Since March 2021, it continuously surveys the northern sky with field of view ~ 2 sr and >90% duty cycle. Using 508 days data collected by full array of LHAASO-WCDA, 69 sources were detected significantly, including 5 extra-galactic sources. 19 of these sources have no known TeV counterpart within 0.5 degree. In this paper, detailed analysis will be presented including background estimation, searching strategy and summary of the catalog.

38th International Cosmic Ray Conference (ICRC2023)
26 July - 3 August, 2023
Nagoya, Japan

ICRC2023
38th International Cosmic Ray Conference
The Astroparticle Physics Conference

*Speaker

PoS(ICRC2023)655

1. Introduction

Gamma rays are one of the most important messengers of the non-thermal universe. The main goal of very high energy gamma astronomy is to find the origin of very high energy cosmic rays: on the one hand, the possible acceleration region of cosmic rays can be studied through discrete gamma ray sources; on the other hand, the interaction of cosmic ray particles with the interstellar medium, interstellar magnetic field or radiation field during propagation can be studied through the spatial distribution and energy spectrum of diffuse gamma.

Catalog analysis is an important way to discover new sources and show the capability of detectors. In recent years, with the upgrading of detection arrays and the improvement of sensitivity, many experiments have conducted source surveys on the galactic plane and even the north sky region, and a number of new sources have been discovered. The HAWC experiment published its second (2HWC) [2] and third (3HWC) catalogs [3] in 2017 and 2020, respectively. Based on 1,523 days of data, 3HWC reported 65 sources, 20 of which had no known TeV sources within 1 degree of their surroundings. The source search strategy adopted by 2HWC and 3HWC is similar: searching for discrete significance peaks with significance greater than 5. The H.E.S.S. Galactic plane survey (HGPS) used about 2,700 hours of data to scan the Galactic plane ($l > 250°$ or $l < 65°$, $|b| < 3°$) and discovered 78 sources, including 16 new TeV sources[1].

With reference to HAWC and HESS search strategies, we develop a search method based on sliding window method, which is more suitable for ground particle arrays with relatively poor angular resolution. Based on LHAASO-WCDA 508 days of data, we did a search analysis of the northern sky. This article will mainly outline the search methods and results.

2. Data Analysis

2.1 LHAASO-WCDA Detector and Data

LHAASO is a composite detection array, designed for the study of CRs and gamma rays across a wide energy range[7]. It consists of three interconnected detector arrays, a 78,000 m^2 Water Cherenkov Detector Array (WCDA) for gamma-ray detection from sub-TeV to multi-TeV, a 1.3 km2 array (KM2A) for gamma-ray detection from 10TeV to beyond 1 PeV, and a Wide Field-of-view Cherenkov Telescopes Array (WFCTA) mainly for CR physics.

As shown in Fig.1, LHAASO-WCDA consists of three ponds with a total of 3,120 detector units. Each detector unit is $5m \times 5m$ and is equipped with two upward-facing PMTs (8-inch and 1.5 inch PMT combination for WCDA-1) on the bottom at the center of the unit. To further lower the threshold energy, WCDA-2 and WCDA-3 employ a 20-inch and 3-inch PMT combination. Each pond is filled with purified water up to 4 m above the PMT photo-cathodes. The results presented here were obtained using the full-array configuration from 2021 March 5 to 2022 September 30. To ensure a reliable data sample, data quality checks were performed based on the DAQ data status and reconstruction quality. The number of gamma-like events recorded by LHAASO-WCDA is around 1.29×10^9 events after event selection and gammaray/background discrimination cuts. The total significance of Crab is 270σ, as shown in Fig.2. As a comparison, the Crab significance of 1523 days in 3HWC is 189σ[3].

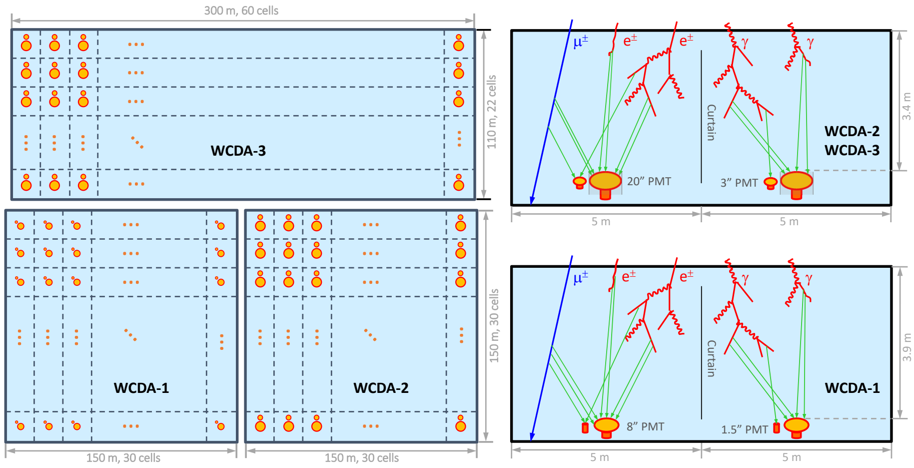

Figure 1: LHAASO-WCDA layout and schematic diagram of the interior layout of the detector unit.

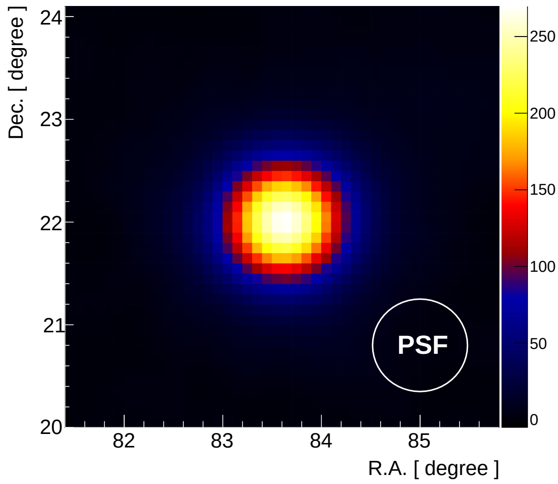

Figure 2: Significance map of Crab nebula based on 508 days of data. The white circle represents the area containing 68% of the signal, with a radius of 0.45 degree.

2.2 Background Estimation and Significance Map

The number of hits in a event, $N_{\rm hit}$, is divided into five segments [100, 200), [200, 300), [300, 500), [500, 800) and [800, 2000]. It is estimated that the covered energy range is from 1TeV to 25TeV according to the position and energy spectrum of Crab. The sky map in celestial coordinates (right ascension and declination) are divided into $0.1^\circ \times 0.1^\circ$ pixels. To obtain the excess of gamma-ray induced showers in each pixel, the "direct integration method"[6] is adopted to estimate the number of background events. The galactic plane are masked to eliminate influence of gamma-ray events on background estimation. Bright sources that are far away from the galactic plane or have a large extension are also masked off.

In the galactic plane, diffuse emission resulting from the interaction of CRs with the interstellar medium and background photons is an essential component of the VHE gamma-ray sky. Such emission has already been clearly detected using the LHAASO data[4]. Therefore, the Galactic diffuse emission (GDE) is also an essential background. However, the GDE is complex and position dependent due to the variation of column density and CR density across the Galaxy. It is not possible to completely disentangle the GDE. To simplify the analysis, the flux morphology of GDE is assumed to follow the spatial distribution of dust measured by Planck maps of dust optical depth[8, 9]. The spectral function is assumed to be identical in all regions. To avoid the influence of the gamma-ray sources, the spectrum of GDE is estimated using the region of Galactic latitude $5^\circ \leq |b| \leq 10^\circ$ and then extrapolated to other Galactic plane regions ($|b| < 5^\circ$). We add the GDE maps detected by LHAASO to the background maps above for subsequent analysis.

A likelihood ratio test is performed between the background-only model and the one point source model to calculate the significance of excess centered at each pixel. The test statistic (TS), defined as $TS = 2ln(L/L_0)$, where L_0 is the maximum likelihood value for the null hypothesis and L is the maximum value for the source hypothesis, is used to estimate the significance. In this work, a power-law spectrum is assumed with an index of 2.6 as initial conditions. This leaves only one free parameter for the likelihood calculation. According to Wilks'Theorem, the TS follows chi-square distribution with one degree of freedom (dof), and the significance can be estimated with $S = \sqrt{TS}$. Fig.3 shows the significance maps in Galactic coordinates. Most sources on the galactic plane are close to each other or overlap, which leads us to introduce the sliding window method into the search strategy.

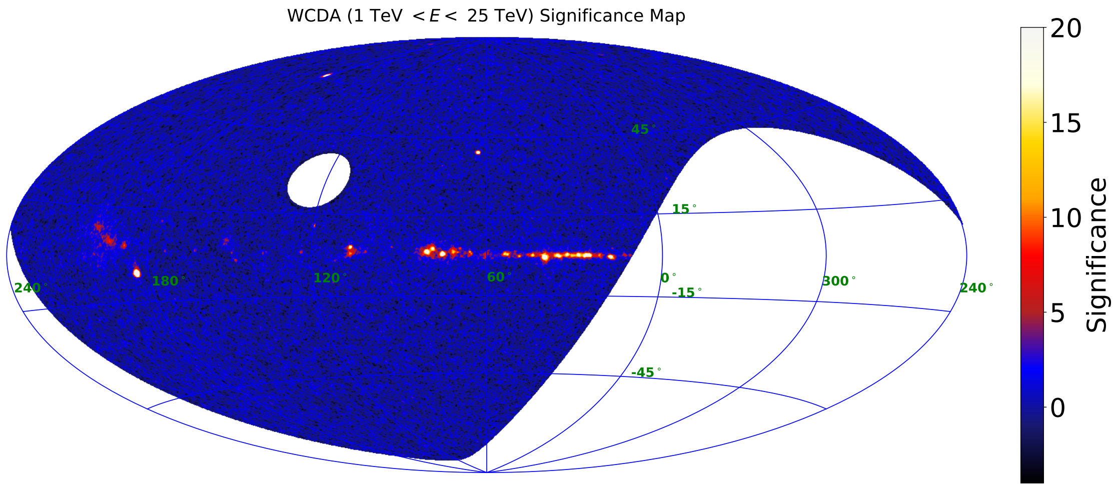

Figure 3: Significance map of the region covered by LHAASO.

3. Construction of The Catalog

Given the density of gamma sources near the galactic plane, especially near the galactic center, the observed signal from a certain direction may come from multiple sources due to the extension of the sources and the limited angular resolution of LHAASO-WCDA. Based on the search methods used by HAWC and H.E.S.S, and combined with the sliding window method, we developed search strategies suitable for LHAASO:

Searching seeds of the source: Based on all-sky $\sqrt{TS}$ map, the search starts with any pixel with significance greater than 5σ, then finds the pixel with the highest significance around it, and take it as the center of the next search area. A search ends when the significance of the pixel in the center of the search area is highest, and the pixel is added to the seeds list. Fig.4 shows the search results.

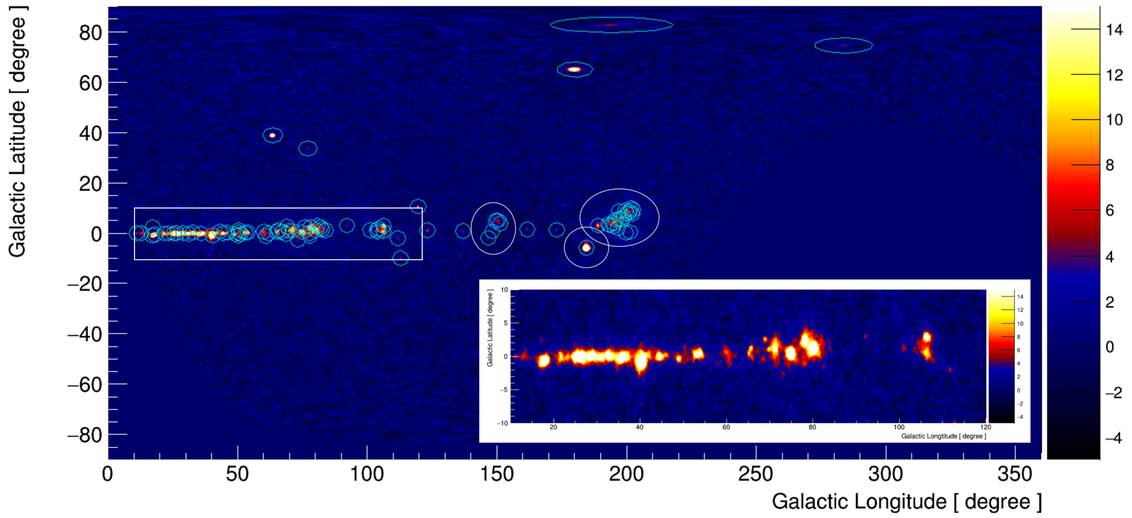

Figure 4: Spatial distribution of seeds on all-sky significance map. The blue circles mark a three-degree radius around each seed. The inserted figure are significance map of part of inner galactic plane.

Demarcating ROI: As can be seen from Fig.4, seeds can be divided into three categories according to the spatial density: Galactic plane region ($10^\circ \leq l \leq 120^\circ$ and $|b| \leq 10^\circ$, referred to as "GP120"), groups of seeds in close proximity (" clusters ", e.g. seeds group near Geminga), and isolated seeds. For GP120, due to very dense sources, the division of ROI cannot meet the requirement in HGPS that the significant excess cannot be located near the ROI boundary. In order to eliminate the large deviation of fitting results caused by the source located at the ROI boundary, a sliding window method was adopted to make overlapping regions between ROIs: the radius of ROIs is 10 degrees, and the sliding step length is the radius of ROI. Except for the GP120 region, the region within three degrees of each seed is set as the territory of that seed. If the territory of a seed does not intersect with the territory of any other seed, the seed is isolated. If they intersect, the two seeds are placed in the same group. For isolated seeds, its territory is taken as ROI of the seed. For a group, the ROI center is defined as the geometric mean of the locations of all seeds in it, and the radius includes areas near all seeds where there are significant excess. The division results of ROI are shown in Fig.5.

Iteration process: For each ROI, starting with one gaussian component, we add gaussian components successively to the source model of each ROI. A likelihood ratio test is used to compare between two models with N and N + 1 Gaussian components. We define $\Delta TS = 2(L_{N+1} - L_N)$. During this iterative process, an additional source characterized by 5 free parameters is added to the model if $\Delta TS > 25$.The iteration process is terminated once no pixel is with TS > 16 in the residual TS map.

Mergence: After the completion of the steps above, all source components determined in each ROI remerged together. Since ROIs can overlap, the same source component could be repeated in

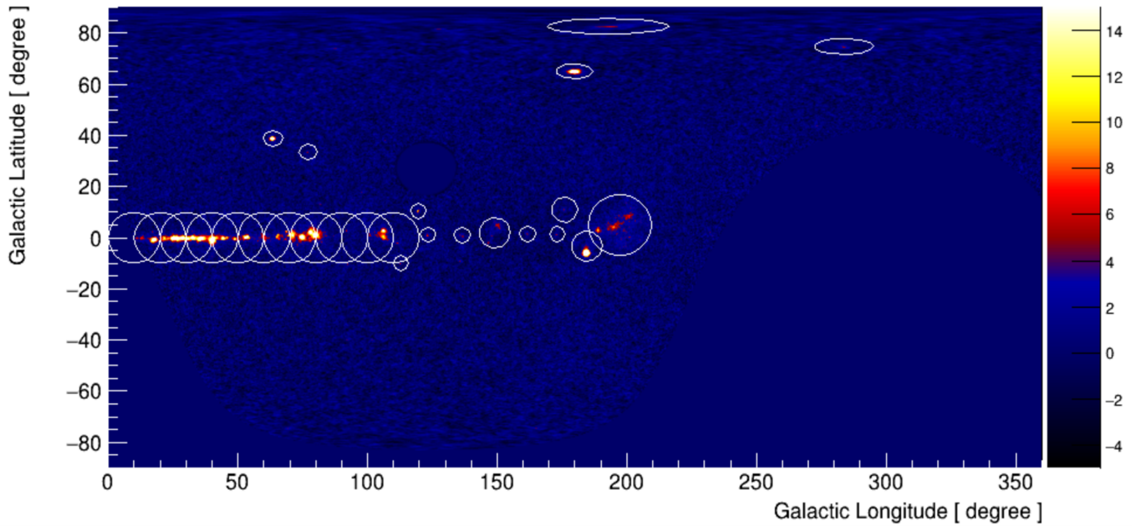

Figure 5: ROIs on all-sky significance map. White circles indicate the areas covered by each ROI.

two adjacent ROIs. In that case, the one closer to the ROI center is selected.

This analysis pipeline yields a preliminary source component list, in which most components have good estimates of parameters. However two possible biases may exist for two cases: 1) the target Gaussian component is close to the ROI edge or a bright source; 2) the iteration fitting scheme described above could converge toward a local maximum. Additional checks have been implemented for these two cases using a new ROI centered on the position of each component and re-analyzing the target source component with free parameters for all components in the ROI.

4. Results

Based on the above data and the diffuse gamma background, the first LHAASO catalog below 25TeV is obtained by using the above search strategy. There are 69 sources with TS greater than 36 and the extension less than 2 degree. Fig.6 shows distribution of spectral index and extension. There are 47 sources with $TS_{\rm ext} > 16$, and 11 sources with spectral index less than 2.0. The complete source list is shown in Tab.1 of [5].

Fig.7 shows the observation of the galactic plane by LHAASO-WCDA. The location and name of the LHAASO-WCDA sources are marked. The name remains the same as in [5], where the "u" means that LHAASO has significant detection of the source above 100TeV. The first LHAASO catalog below 25TeV contains five sources with $|b| > 15°$. In addition to Mrk 421 and Mrk 501, LHAASO-WCDA observations of the remaining three sources are shown in Fig.8. Four of the five sources are spatially associated with known extragalactic TeV sources listed in TeVCat[1]. The remaining one, 1LHAASO J1219+2915, is surrounded by three known extragalactic TeV sources, but all are far away from the source. 1LHAASO J1219+2915 is a point-like source, only detected by LHAASO-WCDA with a significance of $TS = 50.4$, and located at high Galactic Latitude ($b = 82.47°$). We cannot find any pulsar and SNR/PWN counterpart associated with this source.

[1]http://tevcat2.uchicago.edu

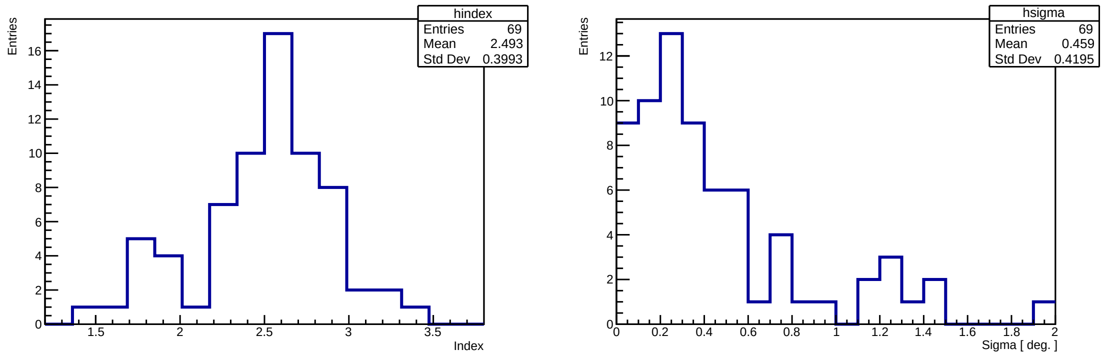

Figure 6: Distribution of spectral index (left) and extension (right) of LHAASO-WCDA sources.

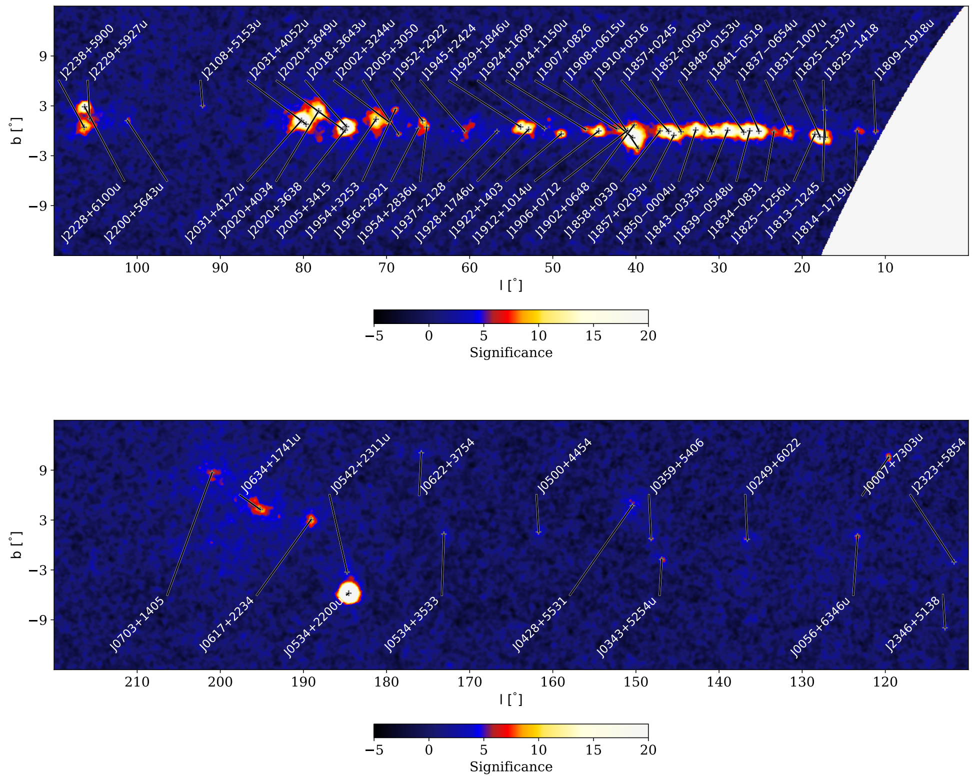

Figure 7: Significance map of part of galactic plane: $0° \leq l \leq 110°$ (top) and $110° \leq l \leq 220°$ (bottom). LHAASO-WCDA sources are represented by black crosses and white labels.

It is a likely extragalactic source due to the high Galactic latitude and null detection by LHAASO-KM2A. The closest AGN counterpart is the Liner-type AGN NGC 4278, at 0.05∘ away from the 1LHAASO source. It is the most possible association even we can not firmly identify this 1LHAASO source at present.

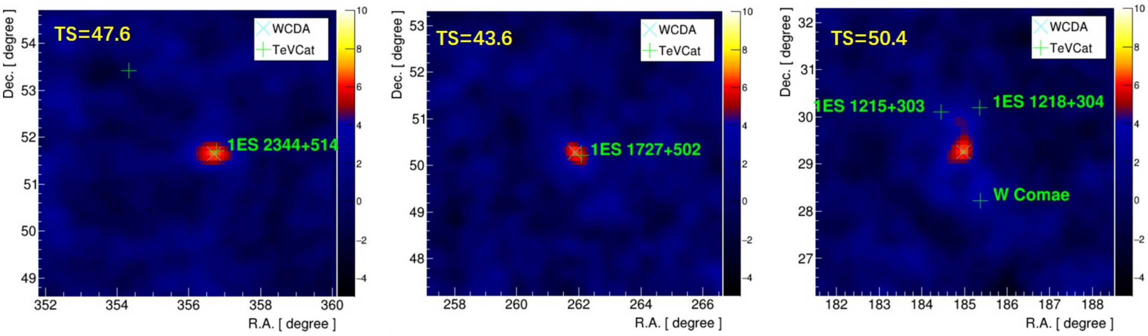

Figure 8: Significance map of three extragalactic sources: 1ES 2344+514 (left), 1ES 1727+502 (middle), new source (right). The position observed by LHAASO-WCDA and that of the surrounding known TeV sources from TeVCat are represented by green and cyan cross, respectively.

References

[1] Abdalla, H., et al. 2018, Astron. Astrophys., 612, A1, doi: 10.1051/0004-6361/201732098

[2] Abeysekara, A. U., Albert, A., Alfaro, R., et al. 2017, The Astrophysical Journal, 843, 40, doi: 10.3847/1538-4357/aa7556

[3] Albert, A., Alfaro, R., Alvarez, C., et al. 2020, The Astrophysical Journal, 905, 76, doi: 10.3847/1538-4357/abc2d8

[4] Cao, Z., Aharonian, F., An, Q., et al. 2023, Measurement of ultra-high-energy diffuse gamma-ray emission of the Galactic plane from 10 TeV to 1 PeV with LHAASO-KM2A. https://arxiv.org/abs/2305.05372

[5] —. 2023, The First LHAASO Catalog of Gamma-Ray Sources. https://arxiv.org/abs/2305.17030

[6] Fleysher, R., Fleysher, L., Nemethy, P., Mincer, A. I., & Haines, T. J. 2004, The Astrophysical Journal, 603, 355, doi: 10.1086/381384

[7] Ma, X.-H., Bi, Y.-J., Cao, Z., et al. 2022, Chinese Physics C, 46, 030001, doi: 10.1088/1674-1137/ac3fa6

[8] Planck Collaboration, Abergel, A., Ade, P. A. R., et al. 2014, , 571, A11, doi: 10.1051/0004-6361/201323195

[9] Planck Collaboration, Aghanim, N., Ashdown, M., et al. 2016, , 596, A109, doi: 10.1051/0004-6361/201629022